CHIN. PHYS. LETT. Vol. 33, No. 8 (2016) 080303

A Realistic Model for Observing Spin-Balanced Fulde–Ferrell Superfluid in Honeycomb Lattices *

Bei-Bing Huang(黄备兵)**

Department of Physics, Yancheng Institute of Technology, Yancheng 224051

(Received 27 March 2016)

The combination of spin–orbit coupling (SOC) and in-plane Zeeman field breaks time-reversal and inversion symmetries of Fermi gases and becomes a popular way to produce single plane wave Fulde–Ferrell (FF) superfluid. However, atom loss and heating related to SOC have impeded the successful observation of FF state until now. In this work, we propose the realization of spin-balanced FF superfluid in a honeycomb lattice without SOC and the Zeeman field. A key ingredient of our scheme is generating complex hopping terms in original honeycomb lattices by periodical driving. In our model the ground state is always the FF state, thus the experimental observation has no need of fine tuning. The other advantages of our scheme are its simplicity and feasibility, and thus may open a new route for observing FF superfluids.

PACS: 03.75.Ss, 05.30.Fk, 67.85.−d DOI: 10.1088/0256-307X/33/8/080303

The inhomogeneous superfluid,[1] including Fulde–Ferrell (FF)[2] and Larkin–Ovchinnikov (LO)[3] superfluid, is a fascinating state proposed to understand the spin-imbalanced fermionic superfluid. In fermionic gases in the absence of spin–orbit coupling (SOC) with large spin imbalance, space inversion symmetry ensures that Cooper pairings with momentum $\boldsymbol{Q}$ and $-\boldsymbol{Q}$ coexist. As a result the LO phase is more favorable than single plane wave FF phase.[4]

The experimental realization of SOC[5–8] dramatically changes this scenario. SOC mixes different spin components and makes the pairings possible on the same Fermi surface even if the spin imbalance exists. Once an in-plane Zeeman field is imposed, which breaks the time-reversal and space inversion symmetries simultaneously, the FF phase rather than the LO phase will have a larger phase space.[9–22] However, the realization of SOC requires near resonant Raman laser and inevitably brings some practical experimental problems such as atom-loss and heating.[23] Due to these obstacles, conclusive evidence of FF states is still elusive.

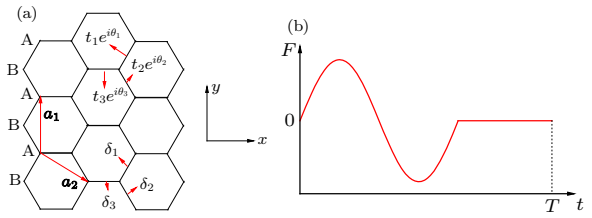

Fig. 1. (a) A schematic diagram of the honeycomb lattice. Here $\boldsymbol{a}_1$ and $\boldsymbol{a}_2$ are basis vectors for the unit cell, $t_\delta e^{i\theta_\delta}$ ($\delta = 1, 2, 3$) are the complex hopping terms along three nearest neighbor directions $\delta_{1,2,3}$. The parameters we assume $\theta_1 = \theta_2 \neq \theta_3$ and $t_1 = t_2 \neq t_3$ can be obtained by periodical driving honeycomb lattice along the x-direction in a specified way. (b) The periodical inertial force induced by driving. An exact period T is shown.

Comparing conventional spin-imbalanced fermionic gases with those with SOC and in-plane Zeeman field, the key ingredient for realizing FF phase is simultaneous breaking of time-reversal and inversion symmetries of the Fermi surface. In this Letter, we suggest an experimentally feasible model without SOC and Zeeman field in the honeycomb lattice to realize single plane wave FF state. Due to the absence of Zeeman field in our model, the FF state proposed here is spin balanced.

We consider a system in a honeycomb lattice. A honeycomb lattice consists of two triangular sublattices denoted by A and B as shown in Fig. 1. The Hamiltonian we study is

$$\begin{aligned} H = &-\sum_{i\delta\sigma} t_\delta [e^{i\theta_\delta} a^\dagger_{i\sigma} b_{i+\delta\sigma} + e^{-i\theta_\delta} b^\dagger_{i+\delta\sigma} a_{i\sigma}] \\ &- U \sum_i [a^\dagger_{i\uparrow} a^\dagger_{i\downarrow} a_{i\downarrow} a_{i\uparrow} + b^\dagger_{i\uparrow} b^\dagger_{i\downarrow} b_{i\downarrow} b_{i\uparrow}] \\ &- \mu \sum_{i\sigma} (a^\dagger_{i\sigma} a_{i\sigma} + b^\dagger_{i\sigma} b_{i\sigma}), \end{aligned} \tag{1}$$

where $a_{i\sigma}$ and $b_{i\sigma}$ denote the fermionic annihilator operators for the sublattices A and B with spin $\sigma = (\uparrow, \downarrow)$, respectively. We choose the basis vectors as $\boldsymbol{a}_1 = (\frac{\sqrt{3}}{2}a, -\frac{a}{2})$, $\boldsymbol{a}_2 = (0, a)$ and three nearest vectors connecting A–B sites as $\delta_1 = \frac{a}{\sqrt{3}}(\frac{1}{2}, \frac{\sqrt{3}}{2})$, $\delta_2 = \frac{a}{\sqrt{3}}(\frac{1}{2}, -\frac{\sqrt{3}}{2})$, $\delta_3 = \frac{a}{\sqrt{3}}(-1, 0)$ with a being the length of the nearest A–A (B–B) sites. Here U (> 0) and μ are on-site attractive interaction strength and chemical potential, respectively. The hopping terms t_δ generally depend on the hopping directions in an anisotropic honeycomb lattice. A feature of our model is phase factors $e^{i\theta_\delta}$ accompanying every hopping. As demonstrated in the following, these phase factors can be induced by periodical driving. Without loss of generality in this work, for simplicity, we assume $\theta_1 = \theta_2 \neq \theta_3$, $t_1 = t_2 = t$ and $t_3 = \lambda t$, where $\lambda > 0$ is the anisotropy parameter. This configuration of phase factors is equivalent to $\theta_1 = \theta_2 = 0 \neq \theta_3$ by a gauge

*Supported by the Natural Science Foundation of Jiangsu Province under Grant No BK20130424, and the National Natural Science Foundation of China under Grant No 11547047.

**Corresponding author. Email: hbb4236@ycit.edu.cn

© 2016 Chinese Physical Society and IOP Publishing Ltd

transformation $a_i \to a_i e^{i\theta_1}$. Usually in some applications sublattice symmetry of honeycomb lattice can be broken by adding such a term $\propto \sum_{i\sigma}(a^\dagger_{i\sigma}a_{i\sigma} - b^\dagger_{i\sigma}b_{i\sigma})$ into the Hamiltonian. In this study we ignore it due to the fact that this term directly gaps out the Dirac point Fermi surface at half-filling.

The model Eq. (1) with all $\theta_\delta = 0$ and $U = 0$ has been realized in experiments and is used to investigate moving and merging of Dirac points by controlling anisotropic parameter λ.[24] When $0 < \lambda < 2$ two Dirac points move in the opposite direction and merge into a semi-Dirac point at $\lambda = 2$, which are featured by a linear-quadratic dispersion relation along different directions. When $\lambda > 2$ the system opens a gap and becomes an insulator, in which the low energy excitation is the massive Dirac fermion.[25]

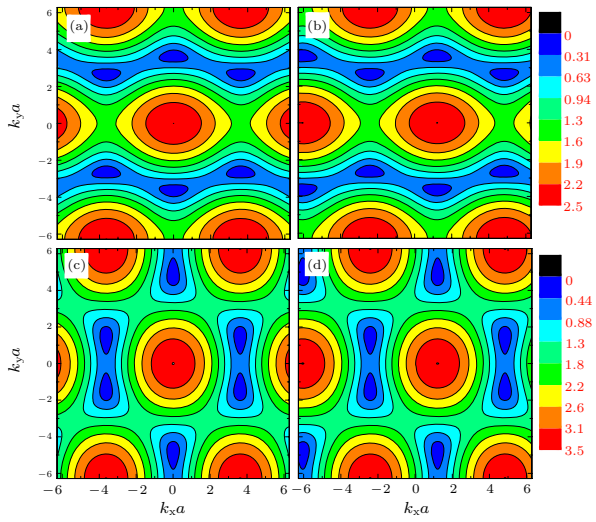

Fig. 2. The upper branch of a single particle spectrum for different anisotropy λ and phase factor θ_3. The parameters are $\lambda = 0.5$, $\theta_3 = 0$ in (a) and $\theta_3 = \pi/3$ in (b), $\lambda = 1.5$, $\theta_3 = 0$ in (c) and $\theta_3 = \pi/3$ in (d). By contrast, the phase factor θ_3 only displaces Dirac points.

The nonzero θ_3 should bring about multiple impacts on the properties of the system. Here we only list two points related to our contents. For real hopping terms the Hamiltonian has a pseudospin symmetry at half-filling,[26] which ensures the degeneracy of the superfluid and charge-density wave (CDW) for an attractive interaction. The complex hopping terms break this symmetry, thus the instability of CDW is very weak in our system. To investigate effects on the single-particle spectrum of nonzero θ_δ, we transform the Hamiltonian into momentum space and obtain

$$E_{\boldsymbol{k}} = \pm t\Big[2 + \lambda^2 + 2\cos k_y a + 4\lambda \cos\frac{k_y a}{2}\cos\Big(\frac{\sqrt{3}}{2}k_x a - \theta_3\Big)\Big]^{1/2}. \quad (2)$$

We find that θ_3 cannot create/annihilate Dirac points by itself but uniformly displaces them as long as $\lambda < 2$. The stability of Dirac points in the presence of θ_3 is protected by the hidden symmetry advocated by Hou *et al.*[27] Additionally, θ_3 also breaks (conserves) time-reversal and inversion symmetries of the system in x- (y-) direction due to $E_{-k_x,k_y} \neq E_{k_x,k_y}$ ($E_{k_x,-k_y} = E_{k_x,k_y}$) (see Fig. 2), which is vital to realize the FF state in our system.

The attractive interaction $-U$ supports pairings among fermions. Due to two separated Fermi surfaces near the half-filling and symmetry breaking caused by θ_3, in principle pairings can happen in the same Fermi surfaces (LO phase) or between two Fermi surfaces (FF phase). There are two factors to impair the stability of LO state. It is easily seen that in the LO phase, pairing momenta have two components for an arbitrary Fermi surface in contrast to the FF phase which only has a nonzero x component due to $E_{k_x,-k_y} = E_{k_x,k_y}$. Extra pairing momentum will increase oscillating behavior of order parameters and kinetic energy of the system. On the other hand in the LO phase, two Fermi surfaces are completely decoupled especially near the half-filling, as a result only half the total density of state determines order parameters for every Fermi surface and the condensation energy is lowered. Thus we only consider the FF state with pairing momentum along the x-direction. Defining mean-field order parameters $\Delta_a = U\sum_{\boldsymbol{k}} < a_{\boldsymbol{Q}/2-\boldsymbol{k},\downarrow}a_{\boldsymbol{Q}/2+\boldsymbol{k},\uparrow} >= \Delta e^{i\varphi}$, $\Delta_b = U\sum_{\boldsymbol{k}} < b_{\boldsymbol{Q}/2-\boldsymbol{k},\downarrow}b_{\boldsymbol{Q}/2+\boldsymbol{k},\uparrow} >= \Delta e^{-i\varphi}$ with FF pairing momentum $\boldsymbol{Q} = (Q_x, 0)$, the mean-field Hamiltonian can be arranged into $H_{\rm mf} = \sum_k[\psi^\dagger_k H_{\rm BdG}(k)\psi_k - 2\mu] + N(|\Delta_a|^2 + |\Delta_b|^2)/U$, with $\psi^\dagger_k = (a^\dagger_{\boldsymbol{Q}/2+\boldsymbol{k},\uparrow}, a_{\boldsymbol{Q}/2-\boldsymbol{k},\downarrow}, b^\dagger_{\boldsymbol{Q}/2+\boldsymbol{k},\uparrow}, b_{\boldsymbol{Q}/2-\boldsymbol{k},\downarrow})$ and

$$H_{\rm BdG}(k) = \begin{pmatrix} -\mu & -\Delta_a & -D(\boldsymbol{k}) & 0 \\ -\Delta_a^* & \mu & 0 & D^*(-\boldsymbol{k}) \\ -D^*(\boldsymbol{k}) & 0 & -\mu & -\Delta_b \\ 0 & D(-\boldsymbol{k}) & -\Delta_b^* & \mu \end{pmatrix}, \quad (3)$$

where $D(\boldsymbol{k}) = \sum_\delta t_\delta e^{i\theta_\delta} e^{i(\boldsymbol{Q}/2+\boldsymbol{k})\cdot\boldsymbol{\delta}}$, and N is the number of unit cell. The Free energy for every unit cell at zero temperature

$$F = \sum_{\boldsymbol{k}}\{-2\mu + \sum_{i=1}^{4}\epsilon_i(\boldsymbol{k})\Theta[-\epsilon_i(\boldsymbol{k})]\} + \frac{|\Delta_a|^2 + |\Delta_b|^2}{U} + \mu n,$$

where $\Theta(x)$ is the Heaviside step function, $\epsilon_i(\boldsymbol{k})$ ($i = 1, \ldots, 4$) are the eigenvalues of $H_{\rm BdG}(k)$, whose exact expressions are too complex to be presented here, and n is the particle density for every unit cell. Here in view of the absence of CDW, particles uniformly distribute in two sublattices and we anticipate that two order parameters have equal magnitude Δ but different phase φ. The order parameters, the relative phase, chemical potential and FF pairing momentum are determined by requiring $\partial F/\partial\Delta = 0$, $\partial F/\partial\varphi = 0$, $\partial F/\partial n = \mu$, and $\partial F/\partial Q_x = 0$.

For model Eq. (1) at half-filling with $\theta_\delta = 0$, the system shows the semimetal-superfluid quantum phase transition when the interaction strength U increases to a critical value $U_c/t \approx 2.13$ at the mean-field level.[28] The existence of this phase transition

depends on vanishing density of state on the Dirac point energy. As nonzero θ_δ cannot annihilate the Dirac points, this quantum phase transition still happens in our model. In this study, we do not involve this phase transition by setting $U/t = 4$. By minimizing the free energy for fixed anisotropy λ and the particle number density n, we always have $Q_x \neq 0$ for $\theta_3 \neq 0$. To further check stability of the FF phase, we also compare the free energy of the FF phase with that of the BCS phase by imposing $\boldsymbol{Q} = 0$. Figure 3(a) shows this difference for $\theta_3 = \pi/6$ and explicitly demonstrates that the FF phase is the true ground state. Since the mean-field Hamiltonian transforms $H_{\rm mf}(\mu) \to H_{\rm mf}(-\mu)$ under particle-hole transformation $a_{i\sigma} \to a^\dagger_{i\overline{\sigma}}$ and $b_{i\sigma} \to -b^\dagger_{i\overline{\sigma}}$ with $\overline{\sigma} = -\sigma$, the free energy has a salient symmetry about half-filling. In Fig. 3(b) we also plot chemical potential as the function of the particle number density for different λ and θ_3, as the compressibility $\kappa^{-1} \propto \partial\mu/\partial n$ is positive. This also illustrates stability of the FF phase. Thus we arrive at our main conclusion that in the presence of complex hopping terms in honeycomb lattices with on-site attractive interaction, BCS state destabilizes and gives way to the FF state.

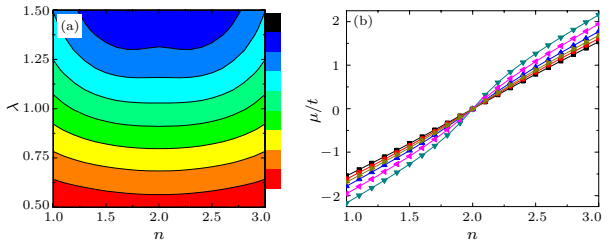

Fig. 3. (a) The difference of free energy between FF and BCS phases for different filling n and anisotropy λ. (b) Chemical potential from self-consistent calculation as the function of filling for different anisotropies $\lambda = 0.5$ (square), $\lambda = 0.8$ (circle), $\lambda = 1.0$ (right triangle), $\lambda = 1.2$ (up triangle), $\lambda = 1.5$ (left triangle) and $\lambda = 1.8$ (down triangle).

In the following we investigate the impact of θ_3 on system properties. Since θ_3 only displaces the Dirac points and does not change density of state on the Fermi surface, it should not affect magnitude of order parameter and chemical potential. This expectation is consistent with numerical results (see Figs. 4(a) and 4(b)). Interestingly the relative phase φ and the FF pairing momentum Q_x show linear behaviors about θ_3 (see Figs. 4(c) and 4(d)), independent of particle number density and anisotropy. We find that this problem can be illustrated easily in pseudospin language.

To use pseudospin, the first step we need to carry out is transforming the $-U$ model Eq. (1) into the $+U$ model, and this can be completed by a partial particle–hole transformation.[29] In this transformed model, the half-filling condition is always satisfied. Thus for small t/U, we obtain the pseudospin exchange model in the second-order perturbative theory as follows:

$$H_{\rm se} = \sum_{i,\delta} H_{i,\delta} - 2\mu \sum_i [T^z_{ia} + T^z_{ib}], \tag{4}$$

with

$$H_{i,\delta} = \frac{4t_\delta^2}{U} T^z_{ia} T^z_{i+\delta b} - \frac{4t_\delta^2}{U} \cos 2\theta_\delta [T^x_{ia} T^x_{i+\delta b} + T^y_{ia} T^y_{i+\delta b}] - \frac{4t_\delta^2}{U} \sin 2\theta_\delta [T^x_{ia} T^y_{i+\delta b} - T^y_{ia} T^x_{i+\delta b}], \tag{5}$$

and pseudospin operators $T^x_{ia} = \frac{1}{2}(a_{i\downarrow} a_{i\uparrow} + a^\dagger_{i\uparrow} a^\dagger_{i\downarrow})$, $T^y_{ia} = \frac{1}{2i}(a^\dagger_{i\uparrow} a^\dagger_{i\downarrow} - a_{i\downarrow} a_{i\uparrow})$, $T^z_{ia} = \frac{1}{2}(a^\dagger_{i\sigma} a_{i\sigma} - 1)$, $T^x_{ib} = \frac{1}{2}(b_{i\downarrow} b_{i\uparrow} + b^\dagger_{i\uparrow} b^\dagger_{i\downarrow})$, $T^y_{ib} = \frac{1}{2i}(b^\dagger_{i\uparrow} b^\dagger_{i\downarrow} - b_{i\downarrow} b_{i\uparrow})$, $T^z_{ib} = \frac{1}{2}(b^\dagger_{i\sigma} b_{i\sigma} - 1)$. In the model Eq. (3), the chemical potential becomes the Zeeman field in the z-direction. When $\mu = \theta_\delta = 0$, this model is reduced to an isotropic antiferromagnetic model by an extra transformation $b_{i\downarrow} \to -b_{i\downarrow}$. If all pseudospins are parallel with the z-axis (x–y plane), this corresponds to the CDW (superfluid) state, while other directions for pseudospins signify mixing of CDW and superfluid. For nonzero θ_δ, $H_{\rm se}$ becomes anisotropic, meanwhile degeneracy between CDW and superfluid is broken as mentioned above.

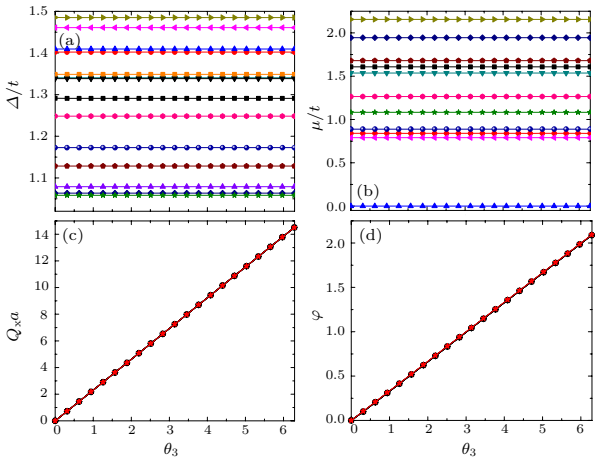

Fig. 4. The impact of phase factor θ_3 on magnitude of order parameter Δ (a), chemical potential μ (b), FF pairing momentum Q_x (c) and relative phase φ (d). In (a) and (b) different lines correspond to different fillings and anisotropies. These two figures signify that Δ and μ do not depend on the θ_3. In (c) and (d), all results from different fillings and anisotropies collapse to the same data points and signify Q_x and φ only depend on θ_3. Two red solid lines in (c) and (d) correspond to the results from pseudospin analysis.

The evolution of superfluid state of model Eq. (1) can be conveniently analyzed in the classical limit of large pseudospin. Replacing pseudospin operators by vectors $\boldsymbol{S}_{ia} = S(\sin\phi_a \cos\varphi_{ia}, \sin\phi_a \sin\varphi_{ia}, \cos\phi_a)$, $\boldsymbol{S}_{ib} = S(\sin\phi_b \cos\varphi_{ib}, \sin\phi_b \sin\varphi_{ib}, \cos\phi_b)$ with $\varphi_{ia,b} = \mp\varphi - \boldsymbol{Q}\cdot\boldsymbol{r}_i$, the classical energy of every unit cell is

$$\frac{E_{\rm cl}}{tS^2} = -\frac{2\overline{\mu}}{S}[\cos\phi_a + \cos\phi_b] + \frac{4}{\overline{U}}(2 + \lambda^2)\cos\phi_a \cos\phi_b - \frac{4}{\overline{U}}\sin\phi_a \sin\phi_b \Big\{2\cos\Big[\frac{Q_x a}{2\sqrt{3}} - 2\varphi\Big]\cos\frac{Q_y a}{2} + \lambda^2 \cos\Big[-\frac{Q_x a}{\sqrt{3}} - 2\varphi + 2\theta_3\Big]\Big\},$$

with $\overline{\mu} = \mu/t$, $\overline{U} = U/t$. The minimization for Q_x, Q_y and φ leads to $Q_x a = 4\theta_3/\sqrt{3}$, $Q_y = 0$, $\varphi = \theta_3/3$. This result is completely consistent with the mean-field numerical result (see solid lines in Figs. 4(c) and 4(d)). Thus the classical energy becomes

$$\frac{E_{\rm cl}}{tS^2} = -\frac{2\overline{\mu}}{S}[\cos\phi_a + \cos\phi_b] + \frac{4}{\overline{U}}(2+\lambda^2)\cos[\phi_a + \phi_b]$$

and does not depend on θ_δ. This also illustrates independence of order parameters and chemical potential of θ_δ in Figs. 4(a) and 4(b). Generally pseudospin analysis only adapts to strong coupling. However for our case $U/t = 4$, strong coupling results can be applied. The minimization for ϕ_a and ϕ_b leads to $\phi_a = \phi_b = 0$ for $\overline{\mu} > 4S(2+\lambda^2)/\overline{U}$ and $\phi_a = \phi_b = \pi$ for $\overline{\mu} < -4S(2+\lambda^2)/\overline{U}$. Otherwise $\cos\phi_a = \cos\phi_b = \overline{\mu}\overline{U}/[4S(2+\lambda^2)]$. Here $\phi_a = \phi_b$ signifies uniform distribution of particle density and absence of CDW.

The model Eq. (1) is available experimentally starting from an isotropic honeycomb lattice. To obtain complex hopping terms, we shake the lattice in a particular way specified in Ref. [30] (see Fig. 1(b)). If the shaking period is the shortest timescale, in the co-moving frame a static effective Hamiltonian can be obtained from the Floquet theory.[31] Compared with the undriven model, the hopping terms in the effective Hamiltonian are renormalized to different values depending on relative direction between hopping and shaking.[30] If shaking is along the x-direction, we will obtain $\theta_1 = \theta_2 \neq \theta_3$ and $t_1 = t_2 \neq t_3$ required in this study. Here we should mention that in the experiment θ_1, θ_2, θ_3 are not equal to zero simultaneously. However our conclusions calculated by requiring $\theta_1 = \theta_2 = 0 \neq \theta_3$ can be directly used to illustrate the experiment as long as the corresponding observables are invariant under the gauge transformation $a_i = a_i e^{i\theta_1}$. In particular, this gauge transformation cannot qualitatively change the pairing property of the ground state.

At the exact half-filling, the Fermi surface of model Eq. (1) is composed of two separated Dirac points for any θ_3 as long as $\lambda < 2$. For nonzero θ_3 time-reversal and inversion symmetries are broken and pairings between two Dirac points definitely carry nonzero momentum, realizing the FF state. Away from the half filling, the point Fermi surface evolves into Fermi lines, reflecting the general characteristic of Fermi surface of the two-dimensional system. As demonstrated, the system remains as the FF state. From this analysis we realize that the FF state in model Eq. (1) does not result from the Dirac point structure of the Fermi surface, but from breaking of time-reversal and inversion symmetries. Thus the mechanism realizing FF state in model Eq. (1) can be extended to other lattices as long as the related symmetries are broken.

A spin-balanced FF state without SOC was also proposed recently by a one-dimensional moving lattice to couple s and p_x bands of cubic optical lattices.[32] In this method the frequency difference of moving lattice must match the band gap between s and p_x bands. To a certain degree, this requires finer tuning than shaking in our model. In addition for a large coupling strength the ground state becomes a BCS superfluid eventually. However in our model, pseudospin analysis suggests that the ground state is still the FF state for arbitrary strong coupling.

In conclusion, we have proposed the realization of a spin-balanced single plane wave FF state in honeycomb lattices with complex hopping terms. It is found that complex hopping terms induce the finite momentum Cooper pairing. Different from some popular suggestions associated with SOC and in-plane Zeeman field, our scheme is much simpler and more feasible experimentally, thus may open a new route for observing FF superfluids.

References

[1] Casalbuoni R and Narduli G 2004 *Rev. Mod. Phys.* **76** 263
[2] Fulde P and Ferrell R A 1964 *Phys. Rev.* **135** A550
[3] Larkin A I and Ovchinnikov Y N 1964 *Zh. Eksp. Teor. Fiz.* **47** 1136
[4] Loh Y L and Trivedi N 2010 *Phys. Rev. Lett.* **104** 165302
[5] Zhang J Y et al 2012 *Phys. Rev. Lett.* **109** 115301
[6] Cheuk L W et al 2012 *Phys. Rev. Lett.* **109** 095302
[7] Wang P et al 2012 *Phys. Rev. Lett.* **109** 095301
[8] Huang L et al 2016 *Nat. Phys.* **12** 540
[9] Zheng Z et al 2013 *Phys. Rev.* A **87** 031602
[10] Zheng Z et al 2014 *Sci. Rep.* **4** 6535
[11] Xu Y, Qu C, Gong M and Zhang C 2014 *Phys. Rev.* A **89** 013607
[12] Wu F, Guo G C, Zhang W and Yi W 2013 *Phys. Rev. Lett.* **110** 110401
[13] Cao Y et al 2015 *Phys. Rev.* A **91** 023609
[14] Qu C et al 2013 *Nat. Commun.* **4** 2710
[15] Zhang W and Yi W 2013 *Nat. Commun.* **4** 2711
[16] Cao Y et al 2014 *Phys. Rev. Lett.* **113** 115302
[17] Chan C F and Gong M 2014 *Phys. Rev.* B **89** 174501
[18] Hu H et al 2014 *Phys. Rev.* A **90** 033624
[19] Liu X J, Hu H and Pu H 2015 *Chin. Phys.* B **24** 050502
[20] Hu H and Liu X J 2013 *New J. Phys.* **15** 093037
[21] Liu X J and Hu H 2013 *Phys. Rev.* A **87** 051608
[22] Zhou X F, Guo G C, Zhang W and Yi W 2013 *Phys. Rev.* A **87** 063606
[23] Galitski V and Spielman I B 2013 *Nature* **494** 49
[24] Tarruell L et al 2012 *Nature* **483** 302
[25] Zhu S L, Wang B and Duan L M 2007 *Phys. Rev. Lett.* **98** 260402
[26] Zhang S 1990 *Phys. Rev. Lett.* **65** 120
[27] Hou J M and Chen W 2015 *Sci. Rep.* **5** 17571
[28] Zhao E and Paramekanti A 2006 *Phys. Rev. Lett.* **97** 230404
[29] Robaszkiewicz S, Micnas R and Chao K A 1981 *Phys. Rev.* B **23** 1447
[30] Struck J et al 2012 *Phys. Rev. Lett.* **108** 225304
[31] Hemmerich A 2010 *Phys. Rev.* A **81** 063626
[32] Zheng Z et al 2016 *Phys. Rev. Lett.* **116** 120403